Title

Identification of a mammalian-type phosphatidylglycerol- phosphate phosphatase in Rhodopirellula baltica

Permalink

https://escholarship.org/uc/item/4xp1q0kz

Authors

Teh, Phildrich
Teh, Phildrich

Publication Date

2012

Peer reviewed|Thesis/dissertation

UNIVERSITY OF CALIFORNIA, SAN DIEGO

Identification of A Mammalian-Type Phosphatidylglycerol-phosphate

Phosphatase in *Rhodopirellula baltica*

A thesis submitted in partial satisfaction of the requirements for the degree of

Master of Science

in

Chemistry

by

Phildrich Teh

Committee in charge:

    Professor Jack Dixon, Chair
    Professor Alexandra Newton
    Professor Susan Taylor

2012

The Thesis of Phildrich Teh is approved and it is acceptable in quality and form for publication on microfilm and electronically:

_____

_____

_____
Chair

University of California, San Diego

2012

TABLE OF CONTENTS

LIST OF FIGURES

ACKNOWLEDGEMENTS

ABSTRACT OF THE THESIS

Identification of A Mammalian-Type Phosphatidylglycerol-phosphate

Phosphatase in *Rhodopirellula baltica*

by

Phildrich Teh

Master of Science in Chemistry

University of California, San Diego, 2012

Professor Jack Dixon, Chair

Cardiolipin, a glycerophospholipid with unique dimeric structure, is predominantly found in the mitochondrial membranes of eukaryotes and the membranes of bacteria. Cardiolipin interacts with protein complexes and plays pivotal roles in cellular energy metabolism, membrane dynamics, and stress responses. Recently, we identified the mitochondrial phosphatase, PTPMT1, as the enzyme responsible for catalyzing the conversion of phosphatidylglycerol-phosphate (PGP) to phosphatidylglycerol (PG), the penultimate step in the *de*

novo biosynthesis of cardiolipin. Using phylogenomic analysis, we examined the evolutionary conservation of PTPMT1 and other cardiolipin biosynthetic enzymes. Our search identified a PTPMT1-like phosphatase in the bacterium *Rhodopirellula baltica* that could dephosphorylate PGP *in vitro*. Its expression restored cardiolipin deficiency and reversed growth impairment in *Saccharomyces cerevisiae* mutants lacking the yeast PGP phosphatase. When ectopically expressed, the bacterial PGP phosphatase localized to the mitochondria of yeast and mammalian cells. This suggests that the N-terminus of the *R. baltica* ortholog can be used as a mitochondrial targeting sequence in eukaryotes. Together, our study demonstrates the conservation of function between bacterial and mammalian PTPMT1 orthologs and establishes an approach to investigate the function of other cardiolipin enzymes in parasitic organisms.

I.

INTRODUCTION

Reversible phosphorylation is a dynamic process that is vital for the regulation of many cellular signaling events (Hunter, 1987; Mustelin *et al.*, 2002). Key participants in maintaining this equilibrium are kinases, which catalyze the transfer of the γ-phosphate from ATP to target substrates, and phosphatases, which reverse phosphorylation by hydrolyzing the substrate's phosphoric acid monoesters (Hanks and Hunter, 1995; Barford, 1996).

Unlike the protein kinases, which are derived from a common ancestor, the protein phosphatases have evolved as separate families that are structurally and mechanistically distinct (Tonks, 2006). The largest family, which consists of more than 100 members, is that of the Protein Tyrosine Phosphatase (PTP) superfamily. Enzymes in this family feature the highly conserved Cys-X_5-Arg (CX_5R) active site motif, in which the cysteine participates as the nucleophile essential for catalysis. Biologically, PTPs play a variety of pivotal roles, including maintaining cell shape and motility, facilitating signal transduction between and within cells, and regulating cell processes such as gene transcription and mRNA processing (Alonso *et al.*, 2004). Furthermore, PTPs are involved in coordinating these processes among neighboring cells in embryogenesis, organ development, tissue homeostasis, and the immune system.

PTPs were once thought to exclusively dephosphorylate phosphotyrosine. More recent studies however, have identified several PTPs that can also cleave phosphate from phosphoserine and phosphothreonine. (Fauman and Saper, 1996; Tonks and Neel, 2001). Moreover, non-proteinaceous substrates such as

lipids, RNA and complex carbohydrates have also been demonstrated to be substrates for PTPs (Maehama and Dixon, 1998; Kim *et al.*, 2002; Worby *et al.*, 2006; Tagliabracci *et al.*, 2007). The tumor suppressor PTEN and the carbohydrate binding protein laforin, for example, dephosphorylate phosphoinositides and glycogen respectively. The primary amino acid sequences of these phosphatases vary from the classical tyrosine-specific PTPs and are therefore categorized into a subfamily called the Dual Specificity Phosphatases (DSPs) (Alonso *et al.*, 2004).

We recently characterized a new member of the DSP subfamily called PTPMT1. Interest in this novel protein arose due to its strong active site similarity with PTEN. PTPMT1 is the first identified PTP localized to the mitochondrion, more specifically, it resides in the inner mitochondrial membrane facing the matrix (Pagliarini *et al.*, 2005). Ablation of the *Ptpmt1* gene in mouse embryonic fibroblasts (MEFs) disrupted cell proliferation and growth, inhibited mitochondrial respiration, reduced electron transport chain complexes, and disturbed mitochondrial membrane morphology (Zhang *et al.,* 2011). Moreover, *Ptpmt1*-knockout mice demonstrated embryonic lethality before day E8.5. Taken together, these observations indicate an indispensible role of PTPMT1 for normal cellular function and embryonic development. *In vitro*, PTPMT1 displays poor activity towards phosphoprotein substrates and preferentially dephosphorylates Phosphatidylinositol 5-phosphate (PI5P) (Pagliarini *et al.*, 2004). However, the level of PI5P remains unchanged in cells with PTPMT1 depletion, suggesting that

PI5P is not the endogenous substrate (Pagliarini *et al.*, 2005). These observations, along with PTPMT1's mitochondrial membrane localization, prompted a lipodomic approach to determine its physiological substrate. *Ptptmt1*-null MEFs exhibited a significant accumulation of phosphatidylglycerol-phosphate (PGP) and a concomitant decrease of phosphatidylglycerol (PG) levels in comparison with *Ptpmt1*-flox cells (*Zhang et al.*, 2011). Further analysis revealed that PTPMT1 is the mammalian phosphatase that mediates the conversion of PGP to PG, a step necessary for the *de novo* biosynthesis of cardiolipin (CL).

CL is an anionic glycerophospholipid found in most organisms from bacteria to eukarya (Schlame, 2008). In eukaryotic cells, CL is an essential component of the inner mitochondrial membrane (White and Frerman, 1967; Zinser *et al.*, 1991). It assembles into membrane domains that dynamically interact with protein-protein or protein-lipid complexes and thus regulates the structure and function of the mitochondria (Mileykovskaya and Dowhan, 2009). Specifically, CL stabilizes the assembly of respiratory complexes III/IV and optimizes ATP production (Hoffmann *et al.*, 1994; Zhang *et al.*, 2005). In addition, CL plays a pivotal role in facilitating protein import, regulating mitochondrial fusion, and maintaining the osmotic stability of mitochondrial membranes (Schlame *et al.*, 2000; Shinzawa-Itoh *et al.*, 2007; Joshi *et al.*, 2009). CL is also required for cell survival, as dissociation of cytochrome *c* from CL triggers apoptosis (McMillin and Dowhan, 2002). In yeast and Chinese-hamster ovary (CHO) cells, deficiency of CL results in impaired viability, abnormal mitochondrial

morphology, and defective respiratory electron transport chain activity (Ohtsuka *et al.*, 1993; Jiang *et al.*, 1999; Gohil *et al.*, 2004). In humans, aberrations in CL metabolism have been linked with life-threatening diseases including Barth Syndrome, ischemia and reperfusion, aging, diabetes, and neurodegeneration (Chicco and Sparagna, 2007; Houtkooper and Vaz, 2008).

The synthesis of cardiolipin involves a series of enzyme-catalyzed reactions first described by Eugene Kennedy in the early 1960's **(Fig. 1)** (Kennedy, 1962). At the first committed step, the enzyme PGP synthase (PGS) facilitates the nucleophilic attack of a glycerol-3-phosphate (G3P) on CDP-diacylglycerol (CDP-DAG). This reaction generates PGP, which is then dephosphorylated to PG by a PGP phosphatase (Chang and Kennedy, 1967). Finally, the enzyme cardiolipin synthase (CLS) catalyzes the reaction between PG and another molecule of CDP-DAG to form CL.

Bacteria employ a similar CL biosynthetic pathway. However, unlike the low abundance of CL in eukaryotes, CL is one of the major anionic phospholipids in most Gram-positive and Gram-negative bacteria (Dowhan, 1997; Cronan, 2003). CL levels increase significantly during stationary growth phase, as well as in response to energy deprivation and osmotic stress (Short and White, 1971; Koch *et al.*, 1984; Catucci *et al.*, 2004). In addition, CL in bacteria forms critical interactions with membrane proteins that are involved in energy metabolism and cellular division (Jormakka *et al.*, 2003; Yankovskaya *et al.*, 2003; Matsumoto *et al.*, 2006; Arias-Cartin *et al.*, 2010).

Given the importance of CL for both eukaryotes and prokaryotes, we utilized comparative genomic and phylogenetic analyses to collectively examine the distribution, structure, and evolution of CL synthetic enzymes. Our analyses intriguingly show that bacterial-type PGP synthase (PGS) and CL synthase (CLS) are present in eukaryotic organisms. In addition, our search revealed a putative PTPMT1 ortholog in the bacterium *Rhodopirellula baltica*. We show that this bacterial enzyme indeed functions as a PGP phosphatase and is localized to the mitochondrion when ectopically expressed in yeast or mammalian cells; thus confirming that PTPMT1 is evolutionarily conserved. Together, our results contribute to the understanding of the evolution of CL metabolism and make an argument for the development of novel therapeutic agent against human parasitic pathogens containing unique CL synthesis enzymes.
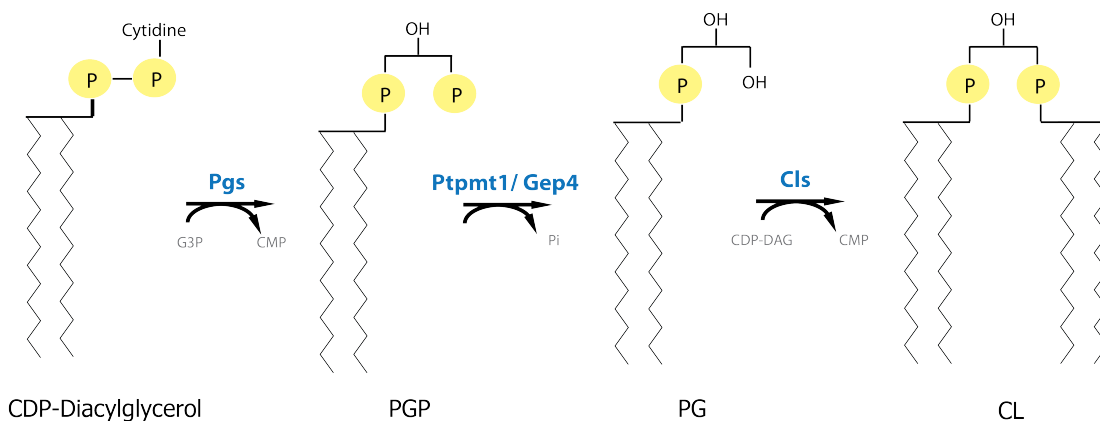
FIG 1. The *de novo* biosynthesis of Cardiolipin in eukaryotes. The first step of the pathway involves the nucleophilic attack of a G3P on CDP-DAG, a process facilitated by the enzyme PGS. The reaction generates PGP, which is then dephosphorylated to PG by either PTPMT1 or Gep4. Finally, the enzyme CLS catalyzes the reaction between PG and another molecule of CDP-DAG to form CL. The depiction above represents the pathway in eukaryotes; however, bacteria share a similar CL synthetic pathway. Enzymes are highlighted in blue.

II.

RESULTS

Phylogenomic Analysis of CL Metabolic Enzymes

To understand the evolutionary conservation of CL, we analyzed the phylogenetic profiles of CL biosynthetic enzymes in more than 30 fully sequenced species selected from all eukaryotic kingdoms and prokaryotic bacteria **(Fig. 2)** (Baldauf, 2003; Keeling *et al*., 2005). Many of these species are known human parasitic pathogens, such as *Entamoeba histolytica*, *Plasmodium falciparum*, *Trypanosoma cruzi*, and *Trichomonas vaginalis*. Using CL metabolic enzymes from *Homo sapiens* as query sequences (or from species specified in the Figure Legends), we performed BLASTp searches to identify putative orthologs in other eukaryotic species and bacteria with cut-off E-values of $<10^{-10}$. Hits that ranked above the threshold were subsequently searched (BLASTp) against the human proteome or that of the specified species. An orthologous gene was identified as the best hit of the bi-directional BLASTp searches and verified by analyzing the domains and motif characteristics. A presence/absence matrix was subsequently obtained based on the BLAST search results **(Fig. 2)**.

In most eukaryotes, the first committed enzyme of the CL biosynthesis pathway PGS, designated here as PGS_euk, contains two PLD-like phosphodiesterase domains **(Fig. 2 and 3A)** (Chang *et al.*, 1998; Kawasaki *et al.*, 1999). A similar catalytic HxKxxxxD motif has been found in several phosphohydrolases and phospholipid synthetases, such as phospholipase D, bacterial phosphatidylserine synthase and CL synthase. Meanwhile, a group of structurally and catalytically distinct enzymes that function as PGS has been discovered in *Arabidopsis* **(Fig. 3A)** (Muller and Frentzen, 2001; Babiychuk *et al.*,

2003). These enzymes belong to the CDP-alcohol phosphatidyltransferase superfamily and exhibit substantial sequence similarity to the bacterial PGS (pgsA), annotated here as PGS_bac (Gopalakrishnan *et al.*, 1986). Interestingly, our phylogenetic analysis identified additional PGS_bac orthologous genes in lower eukaryotes, *T. vaginalis* and *G. lamblia*.

The conversion of PG to CL is also carried out by two types of CLS; eukaryote-like (CLS_euk) and bacteria-like (CLS_bac) (Tian *et al.*, 2012). Similar to the domain structure of PGS_bac, CLS_euk enzymes have a CDP-alcohol phosphatidyltransferase domain. On the other hand, CLS_bac contains two PLD-like domains analogous to those of PGS_euk **(Fig. 3B)** (Serricchio and Butikofer, 2012; Chen *et al.*, 2006). Consistent with the conserved function of CL across evolution, our phylogenetic analyses revealed that CLS_euk is present in most species **(Fig. 2)**. In contrast, the distribution of CLS_bac is more restricted. Noteworthy however, is the presence of this bacterial-type enzyme in several human parasitic pathogens.

The identification of PGS and CLS with both eukaryotic and bacterial-origins prompted us to examine the evolutionary history of PGP phosphatases in detail. Previously, Raetz *et al.* identified three bacterial PGP phosphatases, pgpA, pgpB, and pgpC in *Escherichia coli* (Icho and Raetz, 1983; Funk *et al.*, 1992; Lu *et al.*, 2010) **(Fig. 3C)**. In 2010, Osman et al. reported yet another PGP phosphatase characterized in yeast called Gep4 (Osman *et al.*, 2010). Gep4 belongs to the halo-acid dehydrogenase (HAD)-like family of phosphatases and contains a conserved DXDX(T/V) motif within the active site **(Fig. 3C)** (Collet *et*

al., 1998). Orthologs of Gep4 exist in fungi, plants, ciliates, and heterokonts **(Fig. 2)**. Interestingly, none of these earlier PGP phosphatases share any significant domain structure and sequence homology with PTPMT1.

PTPMT1 is a member of the DSP subfamily of PTPs and contains the consensus, CX_5R motif within the active site **(Fig. 3C)** (Pagliarini *et al.*, 2004). Its orthologs exist in many species of opisthokonts, ameobozoa, plantae, chromalveolates, as well as prokaryotic bacteria **(Fig. 2)**. PTPMT1 and GEP4 are mutually exclusive in opisthokonts, but co-exist in many plants and chromalveolates. Notably, no PGP phosphatase has been found in parasitic apicomplexans, *P. falciparum*, *T. gondii*, and *Cryptosporidium parvum*, where both PGS and CLS orthologs can be identified with confidence **(Fig. 2)**. The presence of the first and third enzymes of CL *de novo* synthesis in those species likely indicates the existence of an additional PGP phosphatase (the second enzyme) that is integral for parasitic CL metabolism.

PTPMT1 Orthologs in Prokaryotic Bacteria

Our phylogenetic analysis identified mammalian-type PTPMT1 orthologs in prokaryotes **(Fig. 2)**. Gep4, on the other hand, is not present in any bacterial species. To further investigate the bacterial-origin of PTPMT1, BLAST searches were performed against bacterial genomes and revealed putative PTPMT1 orthologs in several bacteria, including *Rhodopirellula baltica*, *Anaerolinea thermophila and Sorangium cellulosm* **(Fig. 4A)**. These orthologs contain PTPMT1-like features such as a predicted transmembrane domain, a consensus

CX$_5$R motif with basic residues, and a WPD loop known to be important for the formation of the thiophosphoryl intermediate and subsequent hydrolysis (Xiao *et al.,* 2010). Intriguingly, no ortholog of bacterial PGP phosphatases, pgpA, pgpB, and pgpC, was found in these bacteria.

To confirm that these bacterial genes are *bona fide* PTPMT1 orthologs, a phylogenetic tree of human and bacterial DSPs was built using the maximum likelihood method in PHYML **(Fig. 4B)** (Xiao *et al.*, 2010). As expected, PTPMT1 clustered far away from phosphatases that are known to dephosphorylate proteins, like the MAP Kinase Phosphatases (MKPs) (Pearson *et al.*, 2001). But more importantly, the tree depicts how closely the *Rhodopirellula*, along with the *Anaerolinea and Sorangium* orthologs, group with human PTPMT1 instead of the other human DSPs. In contrast, other bacterial DSPs such as YopH, SptP, IphP, and MptpB clustered distantly (highlighted in blue) (Silva and Tabernero; Patel *et al.*, 2005; Aepfelbacher *et al.*, 2007).

The *Rhodopireulla* PTPMT1 Dephosphorylates PGP *In Vitro*

Of the three identified prokaryotic orthologs, we chose to further study the postulated PTPMT1 ortholog in *R. baltica* because it displays the closest sequence similarity (50%) to mammalian PTPMT1 **(Fig. 4A)**. In our analyses, we also looked at the PTPMT1 ortholog in *Drosophila melangoster*. Knockdown of the PTPMT1 ortholog in *Drosophila* has been shown to suppress the neurodegeneration defect in flies bearing a mutation in the Valosin-containing protein (VCP), a hexameric AAA ATPase that participates in a variety of cellular

processes such as protein degradation, organelle biogenesis, and cell-cycle regulation (Chang *et al.*, 2011).

Each gene was individually cloned into Glutathione S-transferase (GST) bacterial expression vectors, expressed, and affinity purified. The pH/rate profiles of these recombinant proteins performed against the artificial phosphotyrosine analog para-nitrophenol (pNPP) were obtained. The *M. musculus*, *D. melangoster*, and *R. baltica* PTPMT1 variants were most efficient at pH 5.5, 7.0, and 8.5, respectively. Subsequently, the specific activities of all orthologs were measured at their respective optimum pH using pNPP as the substrate **(Fig. 5A)**. All PTPMT1 orthologs tested, possessed measurable phosphatase activity against pNPP. In contrast, the catalytically inactive Cysteine to Serine (CS) mutants exhibited no activity. Notably, the specific activity of PTPMT1 orthologs against pNPP are relatively low compared to other PTPs, such as dPTP61F and VHR (Taylor *et al.*, 2000). However, the inability to efficiently dephosphorylate pNPP is shared by other lipid phosphatases, like PTEN and myotubularins.

We next tested whether these orthologs could actually dephosphorylate PGP, the physiological substrate of mammalian PTPMT1. We enzymatically synthesized radiolabeled PGP by incubating sn-[U-^{14}C] glycerol-3-phosphate with CDP-DAG in the presence of purified recombinant PGP synthase from *E. coli*, as illustrated in **Fig. 5B** (Dowhan, 1992; Xiao *et al.*, 2010). The resulting ^{14}C-PGP was then extracted and further incubated with each PTPMT1 ortholog. The reaction mixture components were separated by means of thin-layer chromatography (TLC) and visualized by autoradiography **(Fig. 5C)**. *Drosophila*

and *Rhodopirellula* PTPMT1 successfully converted PGP to PG, similar to that of *M. musculus* PTPMT1 **(Fig. 5C)**. Their CS mutants along with the glucan phosphatase Laforin, displayed no activity towards PGP. Together, our results demonstrate that PTPMT1 orthologs in *Drosophila* and *Rhodopirellula* dephosphorylate PGP *in vitro*.

The *Rhodopirellula* PTPMT1 Functions as a PGP Phosphatase *In Vivo*

To further validate that the *Rhodopirellula* and *Drosophila* PTPMT1 function as PGP phosphatases, we utilized an *in vivo* yeast complementation system. GEP4 has been identified as the PGP phosphatase in yeast and its deletion results in a concomitant increase in PGP along with a reduction of CL levels (Osman *et al*., 2010). Notably, *gep4Δ* cells display significant growth deficiency when grown at elevated temperatures or cultured on media containing ethidium bromide, an agent that induces loss of mitochondrial DNA and defects in the cell wall (Janitor and Subik, 1993).

If PTPMT1 orthologs truly function as PGP phosphatases, they should rescue this *GEP4*-knockout phenotype. Therefore, we complemented *GEP4*-knockout yeast cells with a control plasmid or plasmids encoding either wildtype or catalytically inactive forms of the PTPMT1 orthologs. Indeed, expression of WT PTPMT1 orthologs effectively restored normal growth while expression of their CS mutants failed to complement the loss of GEP4 **(Fig. 6A)**. The expression of PTPMT1 orthologs in yeast was confirmed by western blot analysis using an anti-FLAG M2 antibody **(Fig. 6A)**. Our results indicate that PTPMT1

orthologs from both *Rhodopirellula and Drosophila* serve as functional equivalents of GEP4 in yeast.

To examine the steady-state levels of PGP and CL in yeast, total lipids were extracted from ^{32}P-orthophosphate labeled cells and separated via TLC. As previously reported, a substantial amount of PGP is observed in *gep4Δ* cells, while it is barely detectable in the wildtype **(Fig. 6B)** (Osman *et al*., 2010). The individual complementation of mouse, fly, or bacterial PTPMT1 in *gep4Δ* cells alleviated the accumulation of PGP back to the level in wildtype cells, consistent with their *in vitro* PGP phosphatase activities. CL levels were also restored to normal levels; whereas the CS mutants failed to rescue this defect **(Fig. 6C)**. Taken together, these results indicate that the bacterial and fly PTPMT1 possess PGP phosphatase activity *in vivo* and are crucially involved in maintaining CL levels.

## The *Rhodopirellula* PTPMT1 Localizes to the Mitochondrion of Eukaryotes

To functionally compensate the loss of Gep4 in yeast, bacterial PTPMT1 had to be correctly localized to the mitochondria to access its substrate PGP. The proper targeting of newly synthesized proteins to the mitochondria is often mediated by a 'mitochondrial targeting sequence' (MTS) located within the N-terminal region of the protein and often contains approximately 20 residues (Omura, 1998). Although these peptide signals do not have a conserved primary sequence, they possess common characteristics with a uniform design. They are generally enriched with the positively charged residue arginine, have a high

percentage of leucine and serine, and contain no or very few acidic residues (Roise *et al.*, 1986; von Heijne, 1986). Moreover, the spacing between the residues often allows the formation of an ampiphilic α-helix, with positively charged and hydrophobic residues on the opposite faces. It has been shown that the first 37 amino acids of *M. musculus* PTPMT1 contains a MTS (Pagliarini *et al.*, 2005). When fused to a Green Fluorescent Protein (GFP), these 37 amino acids direct the fluorescent signal exclusively to the mitochondrion. Therefore, we compared the N-terminal regions of *D. melangoster,* and *R. baltica* PTPMT1 orthologs to that of the mouse protein **(Fig. 7A)**. Notably, many basic and hydrophobic residues are conserved among PTPMT1 orthologs. We plotted the amino acids comprising the regions potentially forming amphiphilic helices onto a helical wheel **(Fig. 7B)**. In both *M. musculus* and *R. baltica* PTPMT1, the positive charges grouped on one side, and the hydrophobic residues clustered on the other, thus fitting the MTS model described above.

To determine whether the *Rhodopirellula* PTPMT1 resides in the mitochondria in an *in vivo* setting, we cultured *gep4Δ* yeast cells that were complemented with a plasmid encoding the bacterial ortholog and performed subcellular fractionation. As shown in **Fig. 7C**, the *R. baltica* PTPMT1, along with the *D. melangoster* variant, are highly enriched in the histodenz-gradient purified mitochondria. The purity of each fraction was further validated by the presence of the mitochondrial marker, Porin; endoplasmic reticulum (ER) marker, Calreticulin; and the cytoplasmic marker, Phosphoglycerate kinase 1/ Pgk1. The localization of a bacterial protein to the yeast mitochondria likely indicates the conservation of

MTS across evolution and is consistent with the bacterial origin of mitochondria. We then postulated that the MTS would behave similarly in higher eukaryotes (i.e. mammalian cells). To test our hypothesis, a C-terminal GFP-tagged bacterial PTPMT1 was introduced into COS-1 cells (originated from African green monkey). The mitochondria were subsequently labeled with MitoTracker Red and the cells were fixed for immunofluorescent analysis. A substantial amount of the *R. baltica* PTPMT1 targeted to the mitochondria as indicated by the co-localization of the two fluorescent signals **(Fig. 7D)**. Together, our results suggest that the *R. baltica* PTPMT1 contains a conserved and functional MTS like sequence.
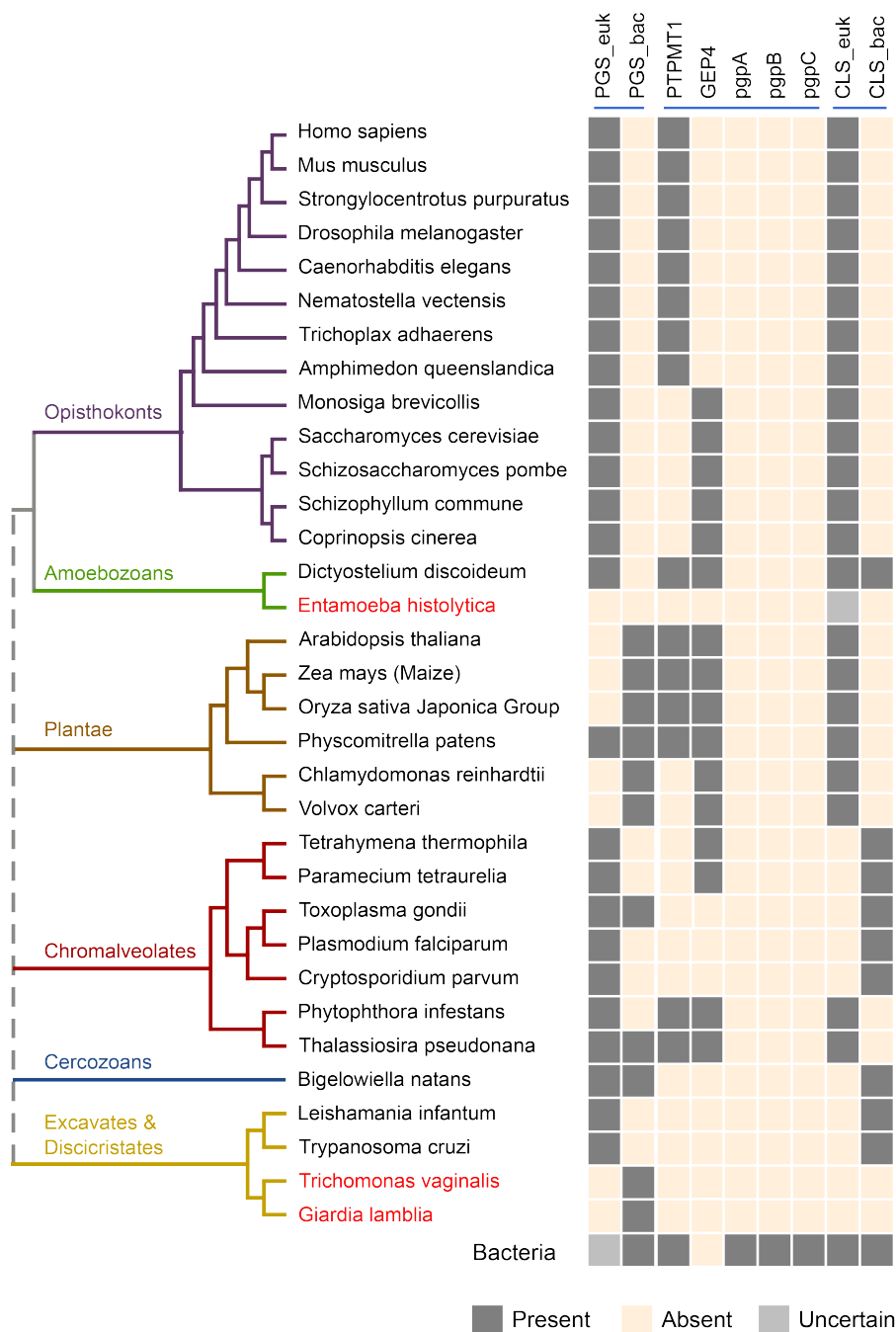
FIG 2. Presence and absence matrix of the CL metabolic enzymes. Dark gray squares indicate presence of CL enzyme (column) in target species (row). Peach squares mean no ortholog has been identified; whereas, light gray squares represent uncertainty when blast search hits are identified but fail to meet the bidirectional-best-hit criterion. The species highlighted in red possesses non-canonical mitochondrion. Sequences of *E. coli* pgsA (PGS_bac), *S. cerevisiae* GEP4, *E. coli* pgpA, pgpB, pgpC, and cls1 (CLS_bac) were used as query for the blast searches. All other enzymes are from *H. sapiens*.
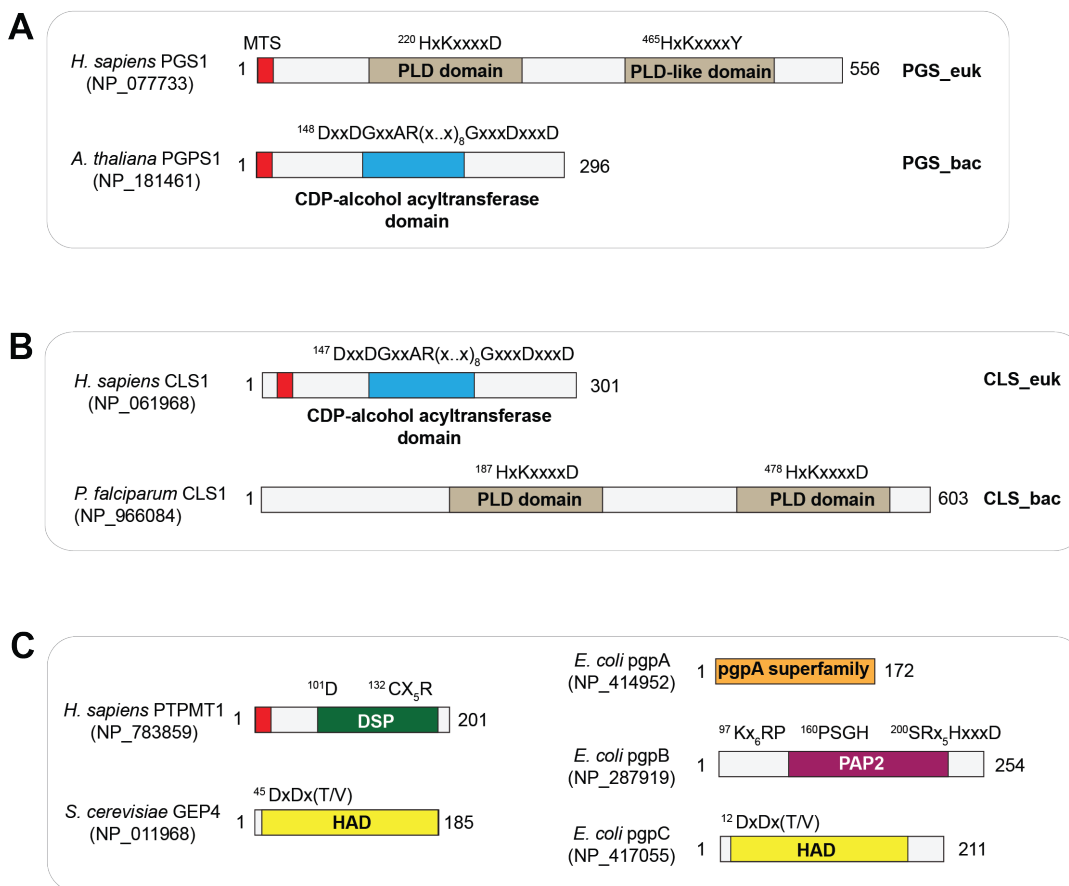
FIG 3. Schematic representation of CL metabolic enzymes. All domains are presented based on analyses using PFAM, CDD, and PROSITE. *A)* Representative PGS_euk and PGS_bac enzymes from *H. sapiens* and *A. thaliana*. MTS, mitochondrial target sequence (red bar); PLD, phospholipase D. The residues involved in catalysis are listed above the diagram. *B)* Representative CLS_euk and CLS_bac from *H. sapiens* and *P. falciparum*. *C)* PGP phosphatases from *H. sapiens*, *S. cerevisiae*, and *E. coli*. DSP, dual specificity phosphatase; HAD, haloacid dehydrogenase; PAP2, phosphatidic acid phosphatase 2.

A

B
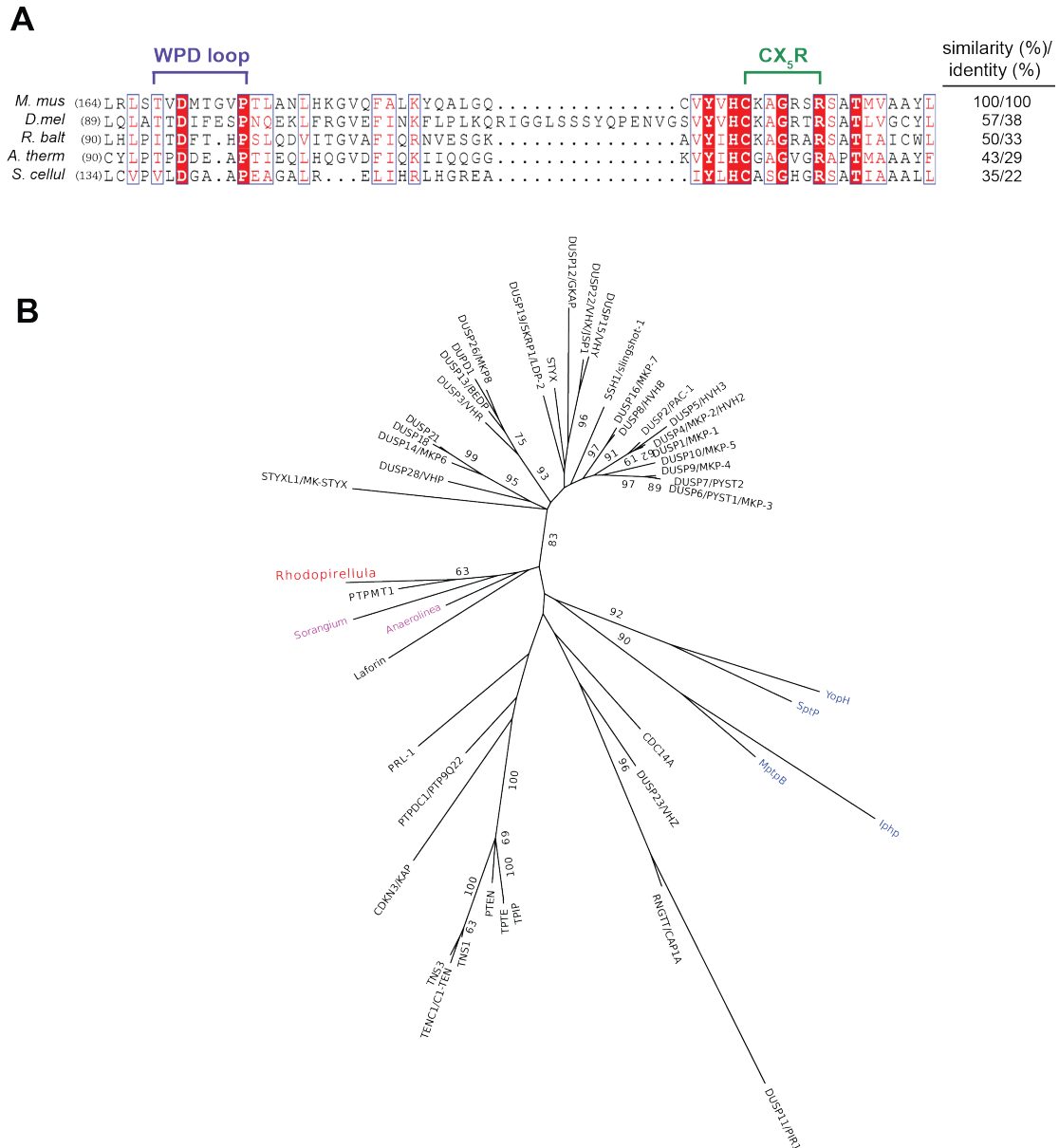
FIG 4. PTPMT1 orthologs in bacteria. *A)* Active site primary sequence alignment of mammalian and bacterial PTPMT1 orthologs using PROMALS3D and illustrated by ESpript (Gouet *et al.*, 1999). Indicated with purple and green bars are the conserved WPD loop and CX$_5$R motifs of the orthologs, respectively. *Mus musculus* (*M. mus*), *Drosophila melangoster* (*D. mel*), *Rhodopirellula balica* (*R. balt*), *Anaerolinea thermophila (A. therm)*, and *Sorangium cellulosm (S. cellul)*. ***B)*** Phylogenetic tree of human and bacterial DSPs constructed using maximum likelihood (ML). *M. mus* PTPMT1 is bolded and bacterial PTPMT1 orthologs are highlighted in red and light purple. Bacterial DSPs unrelated to PTPMT1 are highlighted in blue.
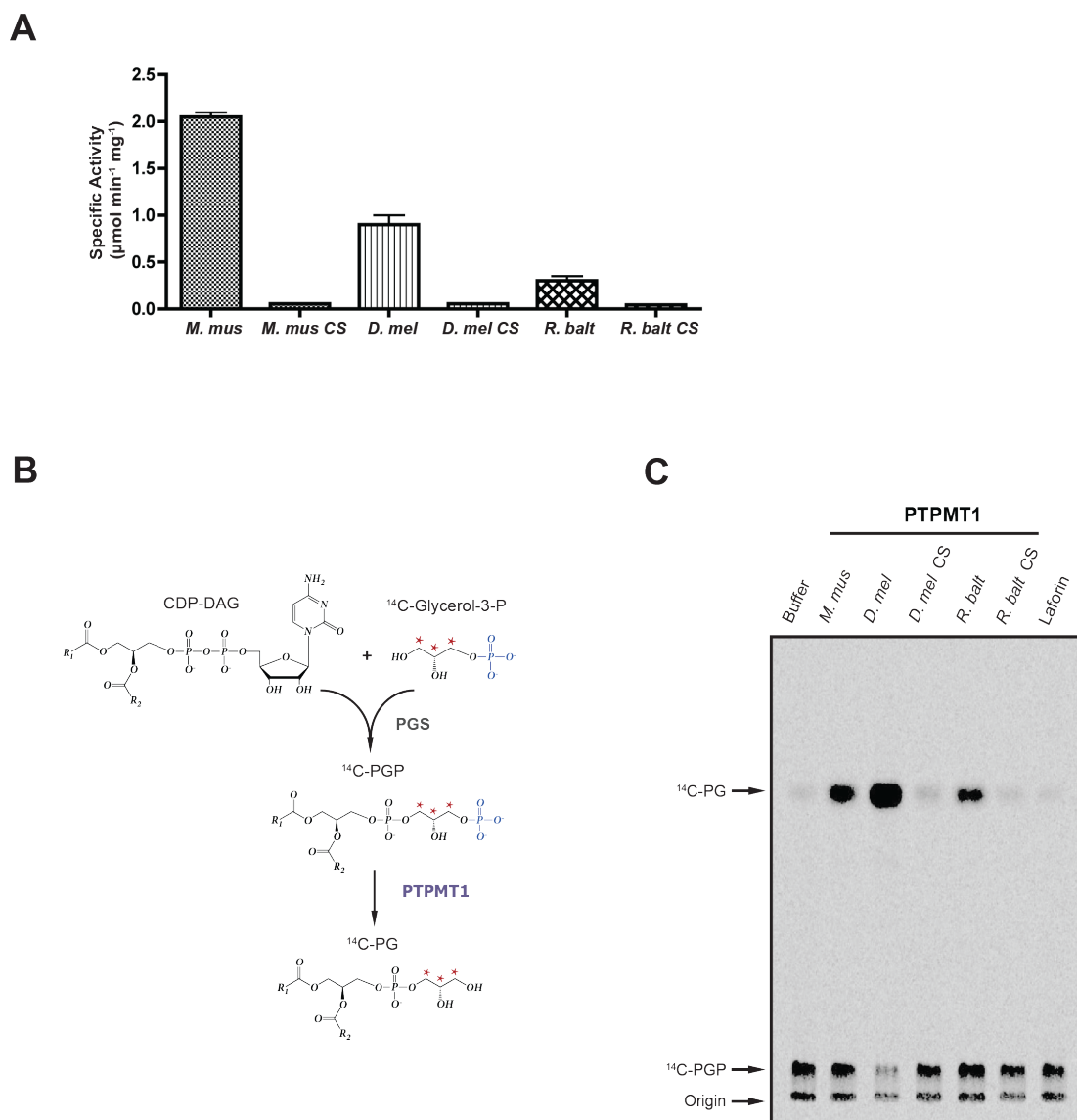
FIG 5. Analysis of the *R. baltica* PTPMT1 activity *in vitro*. A) The specific activities of recombinant murine (*M. mus*), fly (*D. mel*), and bacterial (*R. balt*) PTPMT1 are measured using pNPP as substrate. Data are calculated from the change in absorbance at 410nm and represented as the mean ± SD of triplicate measurements. CS, catalytically inactive mutant. **B)** Synthesis of ^{14}C-PGP and depiction of reaction assay setup. Highlighted in blue is the phosphate group cleaved by PTPMT1 and marked with red asterisks are the radiolabled carbons. **C)** Activities of wild-type and catalytically inactive PTPMT1 orthologs against PGP.

A

B

C
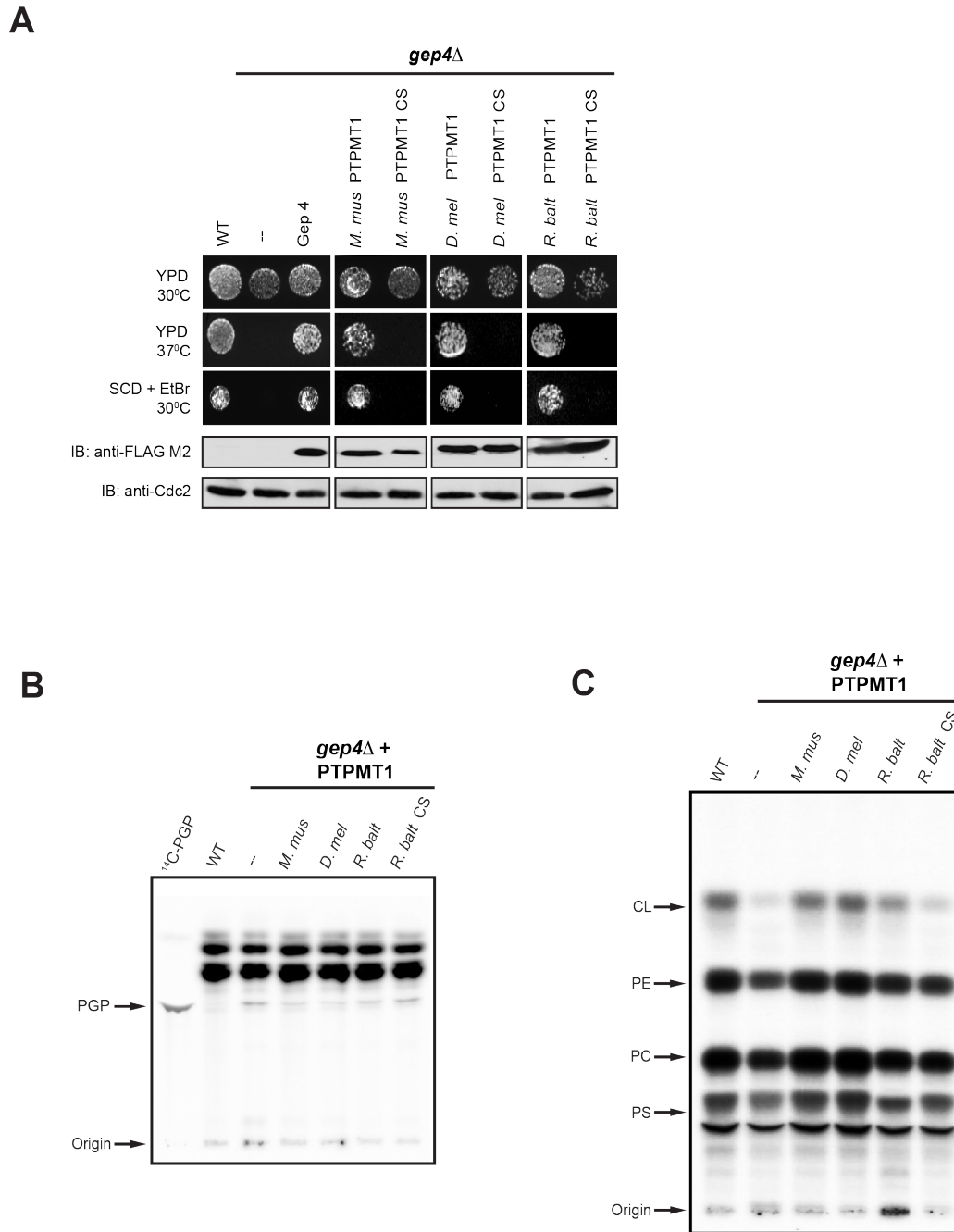
FIG 6. *R. baltica* **PTPMT1 functionally compensates loss of Gep4** *in vivo. A)* Wild-type murine, fly, and bacterial PTPMT1 complement the growth deficiency of *GEP4*-null cells. The expression levels of FLAG-tagged PTPMT1s and GEP4 are indicated by protein immunoblot analysis. CDC2 levels are shown as the loading control. Detection of steady–state PGP *(B)* and CL *(C)* levels in *gep4Δ* yeast cells complemented with control plasmid or plasmids encoding PTPMT1 orthologs. Cells are labeled with ^{32}P at 10µCi/ml for 12 hrs. Lipids are extracted, separated via TLC, and viewed by autoradiography.
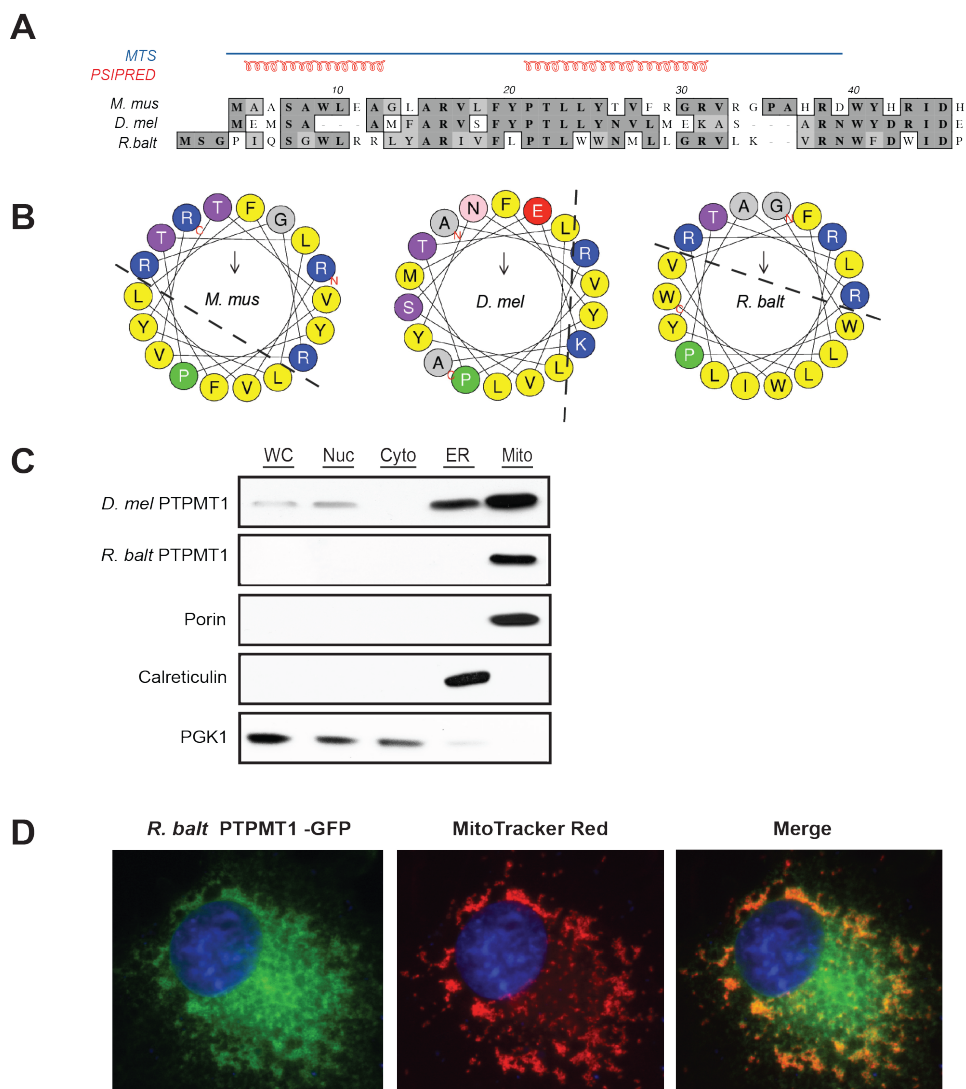
FIG. 7. Mitochondrial localization of the *Rhodopirellula* PTPMT1. A) The N-terminal sequences of PTPMT1 orthologs are aligned using PROMALS3D. Amino acid similarities are shaded in light gray and identities in dark gray. The MTS of mouse PTPMT1 is indicated by the blue bar. The regions of mouse PTPMT1 forming α-helices are predicted by PSIPRED and depicted in red (Buchan *et al.*). **B)** The N-terminal region of bacterial PTPMT1 forms an amphiphilic helix. 18 amino terminal residues are plotted on the helical wheel using HeliQuest (Gautier *et al.*, 2008). Basic residues are colored blue and hydrophobic residues are colored yellow. **C)** Subcellular fractionation of yeast *gep4Δ* cells expressing fly or bacterial PTPMT1. 30μg of each fraction are analyzed by SDS-PAGE and immunoblotting. VDAC, CALR, and PGK1 serve as marker proteins for mitochondria, ER, and cytosol, respectively. **D)** Bacterial PTPMT1 localizes to the mitochondria of mammalian COS-1 cells. 24 hrs. post-transfection, cells are stained with MitoTracker Red, fixed, and analyzed by immunofluorescence imaging.

III.

DISCUSSION

In this study, we examined the phylogenetic distribution of CL metabolic enzymes across major eukaryotic groups and prokaryotes. Our analysis revealed that the prokaryotic *Rhodopirellula baltica* utilizes a PTPMT1-like phosphatase, as opposed to using a yeast (GEP4) or *E. coli* (pgpA, pgpB, or pgpC) phosphatase to catalyze the conversion of PGP to PG. *Rhodopirellula baltica* is predominantly found in terrestrial and marine habitats and is a heterotrophic microorganism that belongs to the bacterial phylum, *Planctomycetales.* Like other plantomycetes, it possesses distinctive features that are highly uncommon among bacteria. *Rhodopirellula* exhibits unusually complex internal structures and partial compartmentalization, including a characteristic ribosome-containing pirellulosome that contains condensed nucleoid DNA (Lindsay *et al.*, 2001; Fuerst and Sagulenko, 2011). The unique eukaryote-like feature of planctomycetes challenges the current hypothesis regarding the origin of eukaryotic organelles (Fuerst and Sagulenko, 2011). Our results showed that *Rhodopirellula* employs a mammalian-type PGP phosphatase that plays an important role in the organism's cardiolipin biosynthesis, consistent with the close relation of planctomycetes to the eukaryotes.

Our phylogenetic profiling also revealed that CL metabolic enzymes are present in most eukaryotes, with the exception of *E. histolytica*, and the related excavates *T. vaginalis*, and *G. lamblia* (**Fig. 2**). These species lack canonical mitochondria, and instead have a degenerated form of this organelle called mitosome (in *E. histolytica* and *G. lamblia*) or hydrogenosome (in *T. vaginalis*)

(Aguilera *et al.*, 2008; van der Giezen, 2009). Both mitosomes and hydrogenosomes lack the machinery for oxidative phosphorylation, heme biosynthesis, and urea cycle. It is not known whether CL is synthesized in these organisms.

Our results also highlight the presence of parasite-specific CL enzymes in several pathogenic eukaryotes. For instance, the malaria-causing *P. falciparum* contains a bacterial-type CLS non-homologous to the human enzyme, making it a potential new target for the treatment of this pandemic disease (**Fig. 2**). Few studies have developed specific inhibitors for the CL metabolic enzymes, largely because of the essentiality of CL across evolution. However, our findings make a case for the development of a new therapeutic regiment with minimal toxicity to the host. A similar strategy could be extended to develop inhibitors for the parasitic-specific CLS in *T. gondii*, *C. parvum, L. infantum*, and *T. cruzi*, and PGS in *T. vaginalis* and *G. lamblia*, which are responsible for various infectious diseases in human, including toxoplasmosis, leishmaniasis, cryptosporadiosis, Chagas disease, trichomonasis and giardiasis. Such a notion is strongly supported by a recent study in *T. brucei*, where genetic disruption of CLS leads to cardiolipin deficiency and parasite death (Serricchio and Butikofer, 2012).

In summary, the phylogenetic analysis presented here allowed us to examine the evolutionary underpinnings of the CL pathway. Our strategy identified a mammalian-type PGP phosphatase in the prokaryotic *R. baltica*. We performed biochemical and gene complementation assays to subsequently

validate our initial search. Notably, the ability of the bacterial phosphatase to target to eukaryotic mitochondria suggests the existence of a conserved mitochondrial targeting sequence. Reconstruction of the evolutionary relationships among CL metabolic enzymes also provided us a useful tool to identify potential anti-parasitic targets for the treatment of malaria and other human parasitic diseases, where standard therapies are often ineffective due to drug resistance or intolerance.

IV.

MATERIALS AND METHODS

Phylogenetic Analysis

The putative orthologs of CL metabolic enzymes in organisms under study were found by reciprocal BLASTp searches using threshold E-value e^{-10}. If no ortholog was found in an organism, the representative sequence was BLASTed and/or PSI-BLAST against protein and nucleotide sequences of that organism and the hits with E-value better than 10 were checked manually. The domain structures of representative CL metabolic enzymes were analyzed using PFAM, CDD, and PROSITE (Punta *et al.,* 2012; Marchler-Bauer *et al.*, 2005; de Castro *et al.*, 2006)

The phylogenetic tree of selected human and bacterial DSPs was built using only the phosphatase domains. Sequences were aligned by PROMALS3D (Pei *et al.*, 2008) and adjusted manually. Phylogenetic trees were inferred using maximum likelihood (ML) and neighbor joining (NJ) methods in MEGA 5.0 (Tamura *et al.,* 2011). Different models of Poisson Correction, Dayhoff matrix, Jones–Taylor–Thornton (JTT) matrix, and JTT + frequency (F) were used, and they are consistent with each other on reliable branches. Support for each interior branch was tested with 100 and 1,000 bootstrap replicates for ML and NJ analyses, respectively.

Protein Expression and Purification

M. musculus, *D. melangoster*, and *R. baltica* PTPMT1 orthologs were each expressed as fusion protein with an N-terminal GST tag in *E. coli* BL21 (DE3) CodonPlus RIPL cells (Strategene). The expression plasmids were

constructed by ligating the PCR products of full-length *PTPMT1 orthologs* into the modified pET41a vector, pSJ6. Cultures were grown at 37 ^{0}C in LB medium to an OD$_{600}$ of 0.6. Cultures were then induced with isopropyl-1-thio-β-D-galactose pyranoside (IPTG) to a final concentration of 0.4mM and allowed to grow overnight at 25 ^{0}C. Cells were collected by centrifugation, resuspended in lysis buffer [25mM Tris pH 8.0, 150mM NaCl, 1mM EDTA, 10% glycerol, 0.5mM TCEP (Tris(2-carboxyethly)phosphine), 1mM Pefabloc SC, 1mM bezamidine-HCl, 1mM PMSF (phenylmethylsulphonyl fluoride)], and lysed using a high pressure homogenizer (Avestatin EmulsiFlex C5). Lysed samples were centrifuged at 43,000 g for 30 min. to remove insoluble material. The resulting supernatants were used to purify the GST-fusion proteins by affinity chromatography using GST-bind resin (Novagen). Fusion proteins were eluted with 50mM Tris pH 8.0, 150mM NaCl, 1mM EDTA, 10% glycerol, and 15mM reduced glutathione. PTPMT1 CS mutants were generated using site-directed mutagenesis and purified similarly.

para-Nitrophenylphosphate (pNPP) Phosphatase Assay

Forty µl of assay buffer [50mM Sodium Acetate, 25mM bis-Tris, 25mM Tris, 50mM pNPP, 0.1µg/µl BSA, 2mM dithiothreitol] was pre-warmed at 30 ^{0}C for 5 min (Taylor *et al.*, 2000). The pH of the assay buffer was set at 5.5 for *M. musculus* PTPMT1; 7.0 for *D. melangoster* PTPMT1; and 8.5 for *R. baltica* PTPMT1. Recombinant enzymes were diluted to 0.2µg/µl in assay buffer without pNPP. Next, 10 µl of the diluted enzymes were added to the pre-warmed assay

buffers and incubated at 30 ^{0}C for 15 min. Reactions were stopped with 200 μl 0.25N NaOH and OD_{410} of the samples were measured.

Synthesis of ^{14}C-PGP

The ^{14}C labeled PGP was synthesized as previously described (Dowhan, 1992). Briefly, the reaction was carried out in the presence of 0.1M Tris-HCl pH 8.0, 0.1% Triton X-100, 0.2mM CDP-DAG (Avanti Polar Lipids), 0.5mM glycerol-3-phosphate (Sigma), and 13μM sn-[U-14C] glycerol-3-phosphate (2-4μCi/ μmol, American Radiolabeled Chemicals). The reaction was enzymatically initiated by the addition of recombinant *E. coli* PGP Synthase and 0.1M $MgCl_2$. After incubation at 37 ^{0}C for 2 h, 0.5 ml of 0.1N HCl in methanol, 1.5 ml of chloroform, and 3.0 ml of 1M $MgCl_2$ were added to stop the reaction. The organic phase was then extracted, dried under vacuum, and stored at -20 ^{0}C.

^{14}C-PGP Phosphatase Assay

^{14}C-PGP was resuspended in 10mM Tris pH 7.4 by means of ice bath sonication for 5 min. 12.5×10^3 CPM of this radiolabeled PGP and 2μg of recombinant PTPMT1 orthologs were then added to assay buffer [50mM Sodium Acetate, 25mM bis-Tris, 25mM Tris, 0.1μg/μl BSA, 2mM dithiothreitol]. Reactions were incubated at 37 ^{0}C for 10 min and quenched by the addition of 0.5 ml of 0.1N HCl in methanol, 1.5 ml of chloroform, and 3.0 ml of 1M $MgCl_2$. Extractions were performed and resulting lipid products were resuspended in chloroform. Whatman silica gel 60 plate was activated by baking for 1 h at 180 ^{0}F under

vacuum conditions. The TLC plate was then spotted with the resuspended lipids, dried for 10 min in a fume hood, and developed in a chamber containing chloroform/methanol/glacial acetic acid (65:25:8). The plate was exposed to a storage phosphor screen and analyzed using a Typhoon 9410 (GE Healthcare).

^{32}P labeling of Yeast cells and Lipid Extraction

The plasmids for complementation assays were assembled by inserting the PCR products of the *PTPMT1* orthologs with a C-terminal FLAG tag into the pRS415-GPD vector (ATCC). *GEP4* knockout yeast strains are derivatives of S288C and obtained from OpenBiosystems (Brachmann *et al.*, 1998). After verification by gene-specific PCR, *gep4Δ* cells were transformed with the plasmids encoding the PTPMT1 orthologs. Cells were grown in YPD at 30 ^{0}C until mid-log phase followed by the addition of radiolabeled ^{32}P to the final concentration of 10μCi/ml for 12 h. Lipids were isolated as previously described (Chang *et al.*, 1998). Briefly, cells were resuspended in a solution of 0.5M NaCl in 0.1N HCl and vortexed with glass beads for 30 min. Lipids were extracted, dried under vacuum, and separated by TLC. For visualizing cardiolipin, Whatman silica gel 60 plates were utilized and prepared as described above. The separating solution used was chloroform/methanol/ammonium hydroxide/water (130:75:2:6). For visualing PGP, HPTLC silica gel 60 plate was utilized and the separating solution used was ethyl acetate/isopropanol/ethanol/ammonium hydroxide/water (12:36:12:7.2:28.8).

Yeast Phenotype Rescue Assay

The *gep4Δ* cells were transformed and grown at 30 ^{0}C to mid-log phase as described above. Cells were counted and serially diluted 5-fold. Each dilution was spotted onto either YPD plates or Synthetic Completed Medium with Dextrose (SCD) in the presence of 25μg/ml ethidium bromide. Plates were incubated for 2 days at the indicated temperatures. For protein immunoblot analysis, 5 OD_{600} of cells were collected by centrifugation and resuspended in 150 μl of 1.85M NaOH with 7.4% BME. Proteins were then precipated by the addition of 345 μl of 50% Trichloroacetic acid. Precipitates were collected by centrifugation at 12,000 g for 5 min. Pellets were washed twice with 1% TCA, dried under vacuum, and resuspended in SDS/PAGE loading buffer.

Mitochondrial Fractionation

500 ml cultures of *gep4Δ* cells transformed with plasmids encoding either the *D. melangoster* or *R. baltica* PTPMT1 were grown in YPD at 30 ^{0}C to OD_{600} of 2. The purified mitochondria were isolated as previously described (Glick and Pon, 1995). Briefly, cells were collected by centrifugation and resuspended in buffer containing 0.1M Tris-SO$_4$ pH 9.4 and 10mM dithiothreitol. Mixtures were incubated for 15 min at 30 ^{0}C. To convert cells into spheroblasts, pellet mixtures were centrifuged at 2,000 g and resuspended in zymolase containing buffer (2.5 mg of Zymolase 20T per gram of yeast was dissolved in buffer A: 20mM potassium phosphate pH 7.4, 1.2M sorbitol) for 30 min at 30 ^{0}C. All the following steps were performed at 4 ^{0}C. Cells were washed twice with buffer A and

resuspended in buffer B (20mM K$^+$MES pH 6.0, 0.6M sorbitol) containing 0.5mM PMSF. Cells were subsequently homogenized with a glass dounce homogenizer with 15 strokes. Resulting mixtures were spun down at 1,500 g for 5 min and supernatants were saved. This step was repeated once more and supernatants were combined. Supernatants were centrifuged at 12,000 g for 10 min and the resulting pellets (crude mitochondria) were brushed gently and resuspended in buffer B. Histodenz solutions (14.5%, 18%, and 35% w/v) were prepared in 2X buffer B. These solutions were gently laid on top of each other in a Beckman ultracentrifuge tube. Resuspended crude mitochondria were added to the Histodenz gradient and centrifuged at 40,000 rpm for 30 min. Light mitochondria formed between the 14.5% and 18% layers while heavy mitochondria pooled between the 18% and 35% layers. Heavy mitochondria were isolated using a Pasteur pipette and washed twice with buffer B.

Immunofluorescence Analysis

The plasmid for the immunofluorescence assay was constructed by ligating the PCR product of *R. baltica PTPMT1* into the pEGFP-N1 vector (Addgene). The plasmid was transfected into kidney-derived COS 1 cells using Fugene (Roche). MitoTracker Red was added to cells in Dulbecco's Modified Eagle Medium (DMEM) to a concentration of 100nM for 30 min before fixation with 3.7% formaldehyde and permeabilization with ice-cold acetone.

REFERENCES

Aepfelbacher, M., Trasak, C., and Ruckdeschel, K. (2007). Effector functions of pathogenic Yersinia species. Thromb Haemost *98*, 521-529.

Aguilera, P., Barry, T., and Tovar, J. (2008). Entamoeba histolytica mitosomes: organelles in search of a function. Exp Parasitol *118*, 10-16.

Alonso, A., Sasin, J., Bottini, N., Friedberg, I., Osterman, A., Godzik, A., Hunter, T., Dixon, J., and Mustelin, T. (2004). Protein tyrosine phosphatases in the human genome. Cell *117*, 699-711.

Arias-Cartin, R., Grimaldi, S., Pommier, J., Lanciano, P., Schaefer, C., Arnoux, P., Giordano, G., Guigliarelli, B., and Magalon, A. (2011). Cardiolipin-based respiratory complex activation in bacteria. Proc Natl Acad Sci U S A *108*, 7781-7786.

Babiychuk, E., Muller, F., Eubel, H., Braun, H.P., Frentzen, M., and Kushnir, S. (2003). Arabidopsis phosphatidylglycerophosphate synthase 1 is essential for chloroplast differentiation, but is dispensable for mitochondrial function. Plant J *33*, 899-909.

Baldauf, S.L. (2003). The deep roots of eukaryotes. Science *300*, 1703-1706.

Barford, D. (1996). Molecular mechanisms of the protein serine/threonine phosphatases. Trends Biochem Sci *21*, 407-412.

Brachmann, C.B., Davies, A., Cost, G.J., Caputo, E., Li, J., Hieter, P., and Boeke, J.D. (1998). Designer deletion strains derived from Saccharomyces cerevisiae S288C: a useful set of strains and plasmids for PCR-mediated gene disruption and other applications. Yeast *14*, 115-132.

Buchan, D.W., Ward, S.M., Lobley, A.E., Nugent, T.C., Bryson, K., and Jones, D.T. Protein annotation and modelling servers at University College London. Nucleic Acids Res *38*, W563-568.

Catucci, L., Depalo, N., Lattanzio, V.M., Agostiano, A., and Corcelli, A. (2004). Neosynthesis of cardiolipin in Rhodobacter sphaeroides under osmotic stress. Biochemistry *43*, 15066-15072.

Chang, S.C., Heacock, P.N., Clancey, C.J., and Dowhan, W. (1998). The PEL1 gene (renamed PGS1) encodes the phosphatidylglycero-phosphate synthase of Saccharomyces cerevisiae. J Biol Chem *273*, 9829-9836.

Chang, Y.C., Hung, W.T., Chang, H.C., Wu, C.L., Chiang, A.S., Jackson, G.R., and Sang, T.K. (2011). Pathogenic VCP/TER94 alleles are dominant actives and

contribute to neurodegeneration by altering cellular ATP level in a Drosophila IBMPFD model. PLoS Genet *7*, e1001288.

Chang, Y.Y., and Kennedy, E.P. (1967). Biosynthesis of phosphatidyl glycerophosphate in Escherichia coli. J Lipid Res *8*, 447-455.

Chen, D., Zhang, X.Y., and Shi, Y. (2006). Identification and functional characterization of hCLS1, a human cardiolipin synthase localized in mitochondria. Biochem J *398*, 169-176.

Chicco, A.J., and Sparagna, G.C. (2007). Role of cardiolipin alterations in mitochondrial dysfunction and disease. Am J Physiol Cell Physiol *292*, C33-44.

Collet, J.F., Stroobant, V., Pirard, M., Delpierre, G., and Van Schaftingen, E. (1998). A new class of phosphotransferases phosphorylated on an aspartate residue in an amino-terminal DXDX(T/V) motif. J Biol Chem *273*, 14107-14112.

Cronan, J.E. (2003). Bacterial membrane lipids: where do we stand? Annu Rev Microbiol *57*, 203-224.

de Castro, E., Sigrist, C.J., Gattiker, A., Bulliard, V., Langendijk-Genevaux, P.S., Gasteiger, E., Bairoch, A., and Hulo, N. (2006). ScanProsite: detection of PROSITE signature matches and ProRule-associated functional and structural residues in proteins. Nucleic Acids Res *34*, W362-365.

Dowhan, W. (1992). Phosphatidylglycerophosphate synthase from Escherichia coli. Methods Enzymol *209*, 313-321.

Dowhan, W. (1997). Molecular basis for membrane phospholipid diversity: why are there so many lipids? Annu Rev Biochem *66*, 199-232.

Fauman, E.B., and Saper, M.A. (1996). Structure and function of the protein tyrosine phosphatases. Trends Biochem Sci *21*, 413-417.

Fuerst, J.A., and Sagulenko, E. (2011). Beyond the bacterium: planctomycetes challenge our concepts of microbial structure and function. Nat Rev Microbiol *9*, 403-413.

Funk, C.R., Zimniak, L., and Dowhan, W. (1992). The pgpA and pgpB genes of Escherichia coli are not essential: evidence for a third phosphatidylglycerophosphate phosphatase. J Bacteriol *174*, 205-213.

Gautier, R., Douguet, D., Antonny, B., and Drin, G. (2008). HELIQUEST: a web server to screen sequences with specific alpha-helical properties. Bioinformatics *24*, 2101-2102.

Glick, B.S., and Pon, L.A. (1995). Isolation of highly purified mitochondria from Saccharomyces cerevisiae. Methods Enzymol *260*, 213-223.

Gohil, V.M., Hayes, P., Matsuyama, S., Schagger, H., Schlame, M., and Greenberg, M.L. (2004). Cardiolipin biosynthesis and mitochondrial respiratory chain function are interdependent. J Biol Chem *279*, 42612-42618.

Gopalakrishnan, A.S., Chen, Y.C., Temkin, M., and Dowhan, W. (1986). Structure and expression of the gene locus encoding the phosphatidylglycerophosphate synthase of Escherichia coli. J Biol Chem *261*, 1329-1338.

Gouet, P., Courcelle, E., Stuart, D.I., and Metoz, F. (1999). ESPript: analysis of multiple sequence alignments in PostScript. Bioinformatics *15*, 305-308.

Hanks, S.K., and Hunter, T. (1995). Protein kinases 6. The eukaryotic protein kinase superfamily: kinase (catalytic) domain structure and classification. FASEB J *9*, 576-596.

Hoffmann, B., Stockl, A., Schlame, M., Beyer, K., and Klingenberg, M. (1994). The reconstituted ADP/ATP carrier activity has an absolute requirement for cardiolipin as shown in cysteine mutants. J Biol Chem *269*, 1940-1944.

Houtkooper, R.H., and Vaz, F.M. (2008). Cardiolipin, the heart of mitochondrial metabolism. Cell Mol Life Sci *65*, 2493-2506.

Hunter, T. (1987). A thousand and one protein kinases. Cell *50*, 823-829.

Icho, T., and Raetz, C.R. (1983). Multiple genes for membrane-bound phosphatases in Escherichia coli and their action on phospholipid precursors. J Bacteriol *153*, 722-730.

Janitor, M., and Subik, J. (1993). Molecular cloning of the PEL1 gene of Saccharomyces cerevisiae that is essential for the viability of petite mutants. Curr Genet *24*, 307-312.

Jiang, F., Ryan, M.T., Schlame, M., Zhao, M., Gu, Z., Klingenberg, M., Pfanner, N., and Greenberg, M.L. (2000). Absence of cardiolipin in the crd1 null mutant results in decreased mitochondrial membrane potential and reduced mitochondrial function. J Biol Chem *275*, 22387-22394.

Jormakka, M., Byrne, B., and Iwata, S. (2003). Formate dehydrogenase--a versatile enzyme in changing environments. Curr Opin Struct Biol *13*, 418-423.

Joshi, A.S., Zhou, J., Gohil, V.M., Chen, S., and Greenberg, M.L. (2009). Cellular functions of cardiolipin in yeast. Biochim Biophys Acta *1793*, 212-218.

Kawasaki, K., Kuge, O., Chang, S.C., Heacock, P.N., Rho, M., Suzuki, K., Nishijima, M., and Dowhan, W. (1999). Isolation of a chinese hamster ovary (CHO) cDNA encoding phosphatidylglycerophosphate (PGP) synthase, expression of which corrects the mitochondrial abnormalities of a PGP synthase-defective mutant of CHO-K1 cells. J Biol Chem *274*, 1828-1834.

Keeling, P.J., Burger, G., Durnford, D.G., Lang, B.F., Lee, R.W., Pearlman, R.E., Roger, A.J., and Gray, M.W. (2005). The tree of eukaryotes. Trends Ecol Evol *20*, 670-676.

Keithly, J.S., Langreth, S.G., Buttle, K.F., and Mannella, C.A. (2005). Electron tomographic and ultrastructural analysis of the Cryptosporidium parvum relict mitochondrion, its associated membranes, and organelles. J Eukaryot Microbiol *52*, 132-140.

Kennedy, E.P. (1962). Harvey Lect Ser *57*, 143-171.

Kim, S.A., Taylor, G.S., Torgersen, K.M., and Dixon, J.E. (2002). Myotubularin and MTMR2, phosphatidylinositol 3-phosphatases mutated in myotubular myopathy and type 4B Charcot-Marie-Tooth disease. J Biol Chem *277*, 4526-4531.

Koch, H.U., Haas, R., and Fischer, W. (1984). The role of lipoteichoic acid biosynthesis in membrane lipid metabolism of growing Staphylococcus aureus. Eur J Biochem *138*, 357-363.

Lindsay, M.R., Webb, R.I., Strous, M., Jetten, M.S., Butler, M.K., Forde, R.J., and Fuerst, J.A. (2001). Cell compartmentalisation in planctomycetes: novel types of structural organisation for the bacterial cell. Arch Microbiol *175*, 413-429.

Lu, Y.H., Guan, Z., Zhao, J., and Raetz, C.R. (2010). Three phosphatidylglycerol-phosphate phosphatases in the inner membrane of Escherichia coli. J Biol Chem *286*, 5506-5518.

Maehama, T., and Dixon, J.E. (1998). The tumor suppressor, PTEN/MMAC1, dephosphorylates the lipid second messenger, phosphatidylinositol 3,4,5-trisphosphate. J Biol Chem *273*, 13375-13378.

Marchler-Bauer, A., Anderson, J.B., Cherukuri, P.F., DeWeese-Scott, C., Geer, L.Y., Gwadz, M., He, S., Hurwitz, D.I., Jackson, J.D., Ke, Z., Lanczycki, C.J., Liebert, C.A., Liu, C., Lu, F., Marchler, G.H., Mullokandov, M., Shoemaker, B.A.,

Simonyan, V., Song, J.S., Thiessen, P.A., Yamashita, R.A., Yin, J.J., Zhang, D., and Bryant, S.H. (2005). CDD: a Conserved Domain Database for protein classification. Nucleic Acids Res *33*, D192-196.

Matsumoto, K., Kusaka, J., Nishibori, A., and Hara, H. (2006). Lipid domains in bacterial membranes. Mol Microbiol *61*, 1110-1117.

McMillin, J.B., and Dowhan, W. (2002). Cardiolipin and apoptosis. Biochim Biophys Acta *1585*, 97-107.

Mileykovskaya, E., and Dowhan, W. (2009). Cardiolipin membrane domains in prokaryotes and eukaryotes. Biochim Biophys Acta *1788*, 2084-2091.

Muller, F., and Frentzen, M. (2001). Phosphatidylglycerophosphate synthases from Arabidopsis thaliana. FEBS Lett *509*, 298-302.

Mustelin, T., Abraham, R.T., Rudd, C.E., Alonso, A., and Merlo, J.J. (2002). Protein tyrosine phosphorylation in T cell signaling. Front Biosci *7*, d918-969.

Ohtsuka, T., Nishijima, M., Suzuki, K., and Akamatsu, Y. (1993). Mitochondrial dysfunction of a cultured Chinese hamster ovary cell mutant deficient in cardiolipin. J Biol Chem *268*, 22914-22919.

Omura, T. (1998). Mitochondria-targeting sequence, a multi-role sorting sequence recognized at all steps of protein import into mitochondria. J Biochem *123*, 1010-1016.

Osman, C., Haag, M., Wieland, F.T., Brugger, B., and Langer, T. (2010). A mitochondrial phosphatase required for cardiolipin biosynthesis: the PGP phosphatase Gep4. EMBO J *29*, 1976-1987.

Pagliarini, D.J., Wiley, S.E., Kimple, M.E., Dixon, J.R., Kelly, P., Worby, C.A., Casey, P.J., and Dixon, J.E. (2005). Involvement of a mitochondrial phosphatase in the regulation of ATP production and insulin secretion in pancreatic beta cells. Mol Cell *19*, 197-207.

Pagliarini, D.J., Worby, C.A., and Dixon, J.E. (2004). A PTEN-like phosphatase with a novel substrate specificity. J Biol Chem *279*, 38590-38596.

Patel, J.C., Rossanese, O.W., and Galan, J.E. (2005). The functional interface between Salmonella and its host cell: opportunities for therapeutic intervention. Trends Pharmacol Sci *26*, 564-570.

Pearson, G., Robinson, F., Beers Gibson, T., Xu, B.E., Karandikar, M., Berman, K., and Cobb, M.H. (2001). Mitogen-activated protein (MAP) kinase pathways: regulation and physiological functions. Endocr Rev *22*, 153-183.

Pei, J., Tang, M., and Grishin, N.V. (2008). PROMALS3D web server for accurate multiple protein sequence and structure alignments. Nucleic Acids Res *36*, W30-34.

Punta, M., Coggill, P.C., Eberhardt, R.Y., Mistry, J., Tate, J., Boursnell, C., Pang, N., Forslund, K., Ceric, G., Clements, J., Heger, A., Holm, L., Sonnhammer, E.L., Eddy, S.R., Bateman, A., and Finn, R.D. (2012). The Pfam protein families database. Nucleic Acids Res *40*, D290-301.

Roise, D., Horvath, S.J., Tomich, J.M., Richards, J.H., and Schatz, G. (1986). A chemically synthesized pre-sequence of an imported mitochondrial protein can form an amphiphilic helix and perturb natural and artificial phospholipid bilayers. EMBO J *5*, 1327-1334.

Schlame, M. (2008). Cardiolipin synthesis for the assembly of bacterial and mitochondrial membranes. J Lipid Res *49*, 1607-1620.

Schlame, M., Rua, D., and Greenberg, M.L. (2000). The biosynthesis and functional role of cardiolipin. Prog Lipid Res *39*, 257-288.

Serricchio, M., and Butikofer, P. (2012). An essential bacterial-type cardiolipin synthase mediates cardiolipin formation in a eukaryote. Proc Natl Acad Sci U S A *109*, E954-961.

Shinzawa-Itoh, K., Aoyama, H., Muramoto, K., Terada, H., Kurauchi, T., Tadehara, Y., Yamasaki, A., Sugimura, T., Kurono, S., Tsujimoto, K., Mizushima, T., Yamashita, E., Tsukihara, T., and Yoshikawa, S. (2007). Structures and physiological roles of 13 integral lipids of bovine heart cytochrome c oxidase. EMBO J *26*, 1713-1725.

Short, S.A., and White, D.C. (1971). Metabolism of phosphatidylglycerol, lysylphosphatidylglycerol, and cardiolipin of Staphylococcus aureus. J Bacteriol *108*, 219-226.

Silva, A.P., and Tabernero, L. (2010). New strategies in fighting TB: targeting Mycobacterium tuberculosis-secreted phosphatases MptpA & MptpB. Future Med Chem *2*, 1325-1337.

Tagliabracci, V.S., Turnbull, J., Wang, W., Girard, J.M., Zhao, X., Skurat, A.V., Delgado-Escueta, A.V., Minassian, B.A., Depaoli-Roach, A.A., and Roach, P.J. (2007). Laforin is a glycogen phosphatase, deficiency of which leads to elevated

phosphorylation of glycogen in vivo. Proc Natl Acad Sci U S A *104*, 19262-19266.

Tamura, K., Peterson, D., Peterson, N., Stecher, G., Nei, M., and Kumar, S. (2011). MEGA5: molecular evolutionary genetics analysis using maximum likelihood, evolutionary distance, and maximum parsimony methods. Mol Biol Evol *28*, 2731-2739.

Taylor, G.S., Maehama, T., and Dixon, J.E. (2000). Myotubularin, a protein tyrosine phosphatase mutated in myotubular myopathy, dephosphorylates the lipid second messenger, phosphatidylinositol 3-phosphate. Proc Natl Acad Sci U S A *97*, 8910-8915.

Tian, H.F., Feng, J.M., and Wen, J.F. (2012). The evolution of cardiolipin biosynthesis and maturation pathways and its implications for the evolution of eukaryotes. BMC Evol Biol *12*, 32.

Tonks, N.K. (2006). Protein tyrosine phosphatases: from genes, to function, to disease. Nat Rev Mol Cell Biol *7*, 833-846.

Tonks, N.K., and Neel, B.G. (2001). Combinatorial control of the specificity of protein tyrosine phosphatases. Curr Opin Cell Biol *13*, 182-195.

van der Giezen, M. (2009). Hydrogenosomes and mitosomes: conservation and evolution of functions. J Eukaryot Microbiol *56*, 221-231.

von Heijne, G. (1986). Mitochondrial targeting sequences may form amphiphilic helices. EMBO J *5*, 1335-1342.

White, D.C., and Frerman, F.E. (1967). Extraction, characterization, and cellular localization of the lipids of Staphylococcus aureus. J Bacteriol *94*, 1854-1867.

Worby, C.A., Gentry, M.S., and Dixon, J.E. (2006). Laforin, a dual specificity phosphatase that dephosphorylates complex carbohydrates. J Biol Chem *281*, 30412-30418.

Xiao, J., Engel, J.L., Zhang, J., Chen, M.J., Manning, G., and Dixon, J.E. (2010). Structural and functional analysis of PTPMT1, a phosphatase required for cardiolipin synthesis. Proc Natl Acad Sci U S A *108*, 11860-11865.

Yankovskaya, V., Horsefield, R., Tornroth, S., Luna-Chavez, C., Miyoshi, H., Leger, C., Byrne, B., Cecchini, G., and Iwata, S. (2003). Architecture of succinate dehydrogenase and reactive oxygen species generation. Science *299*, 700-704.

Zhang, J., Guan, Z., Murphy, A.N., Wiley, S.E., Perkins, G.A., Worby, C.A., Engel, J.L., Heacock, P., Nguyen, O.K., Wang, J.H., Raetz, C.R., Dowhan, W., and Dixon, J.E. (2011). Mitochondrial phosphatase PTPMT1 is essential for cardiolipin biosynthesis. Cell Metab *13*, 690-700.

Zhang, M., Mileykovskaya, E., and Dowhan, W. (2005). Cardiolipin is essential for organization of complexes III and IV into a supercomplex in intact yeast mitochondria. J Biol Chem *280*, 29403-29408.

Zinser, E., Sperka-Gottlieb, C.D., Fasch, E.V., Kohlwein, S.D., Paltauf, F., and Daum, G. (1991). Phospholipid synthesis and lipid composition of subcellular membranes in the unicellular eukaryote Saccharomyces cerevisiae. J Bacteriol *173*, 2026-2034.